OIL TANKER FATIGUE EVALUATION BY DIRECT HYDRO-STRUCTURE COMPUTATIONS - A COMPARISON WITH THE CSR-H APPROACH

Y. Quéméner, K.C. Chen, C.F. Lee & C.H. Huang, *CR Classification Society (CR), Kobe, Japan*

ABSTRACT

This study investigates the fatigue life of longitudinal stiffeners end connections located amidship in a handysize oil tanker. Specifically, the fatigue is evaluated accordingly to the harmonized common structural rules for bulk carriers and oil tankers recently released by the international association of classification societies. This study highlights the margins taken in the rules for the fatigue, especially regarding the loads long term evaluation. Advanced hydro-structure coupling analyses are thus carried out that enable direct hydrodynamic load computations and accurate structural response assessment by finite element analyses. Spectral fatigue analyses are then performed to obtain the fatigue damage. As a result, the fatigue life computed by hydro-structure analyses is significantly smaller than that produced accordingly to the rules. The detailed observation of the results shows that the loads, stresses and fatigue damages as computed by the rules are reduced compared to those assessed by the advanced analyses under the rules assumptions. This study can thus evaluate the margins taken during the rules development regarding the fatigue assessment based on numerous classification societies' experience.

NOMENCLATURE

Abbreviations

EDW = Equivalent Design Wave
RAO = Response Amplitude Operator

Symbols

D = Fatigue damage
f_{mean} = Correction factor for mean stress effect
H_{EDW} = Equivalent design wave height
M_{wv} = Vertical wave bending moment
N_D = Total number of cycles over the ship design life
P = Lateral pressure
T_D = Design life (25 years)
T_F = Fatigue life
$\Delta\sigma_{FS}$ = Reference fatigue stress range
$\Delta\sigma_{HS}$ = Hot spot stress range
σ_{mean} = Mean stress
Φ = Phase angle

1. INTRODUCTION

Fatigue cracking due to cyclic loading is a common mode of damage in ship structure that can be mitigated by proper fabrication procedure and structural design. Recently, the IACS have released the harmonized common structural rules (CSR-H) for bulk carriers and oil tankers [1] that include a fatigue evaluation procedure to verify that the fatigue life of any critical structural detail is at least greater than 25 years. This criterion complies with the newly adopted goal based ship construction standards (GBS) [2].

The GBS requires also to provide the "explanation of the effect of uncertainties/assumptions on fatigue life, highlighting any margins used in fatigue calculations". The IACS has thus released a technical background report [3] that presents a sensitivity analysis for the fatigue evaluation. The report concludes that no margin is explicitly taken, but for the design SN curves that corresponds to 97.7% of survival probability. The rules are also established in such a manner that the "effect on the fatigue damage due to uncertainty in the load and load effects is usually comparable or greater than effects from the uncertainty in the capacity". The hot spot stress calculation method and SN curve measurements have been developed jointly as addressed by Maddox [4], Fricke [5], Lotsberg [6] and [7], and as such the effects of their respective uncertainties are inherently balanced. On the contrary, some assumptions are extremely conservative like the North Atlantic wave environment considered all along the ship life. The IACS [8] shows that most of ships do not operate permanently in such a stringent environment. However, the influence of this assumption on the long term load assessment and thus on the fatigue is not explicitly reported.

Therefore, this study presents a comparison of the fatigue evaluation by the rules and by advanced hydro-structure coupled analyses. The comparison of both results can highlight the margins taken by the rules. Specifically, this study examines the fatigue life of longitudinal stiffeners end

connections located amidship in a handysize oil tanker.

This study consists of five sections. The first section presents the fatigue evaluation procedures by the rules and by the direct structural assessment. The second section presents the hydro-structure modeling. The third section evaluates the hydrodynamic loads by performing seakeeping analyses. The loads are then transferred to the ship finite element model. The fourth section presents the finite element analyses (FEA) performed to extract the RAO of fatigue stress that enables determining the reference fatigue stress range by spectral fatigue analyses. Finally, the fifth section discusses on the fatigue results derived from the reference fatigue stress range obtained following four different methods from the simple application of the rules to the advanced hydro-structure coupled analyses.

2. FATIGUE ASSESSMENT APPROACHES

2.1 RULES FATIGUE ASSESSMENT

This study evaluates the fatigue of the longitudinal stiffeners end connections in the midship section of the considered ship accordingly to the rules. Figure 1 presents the flowchart of the rules fatigue assessment.

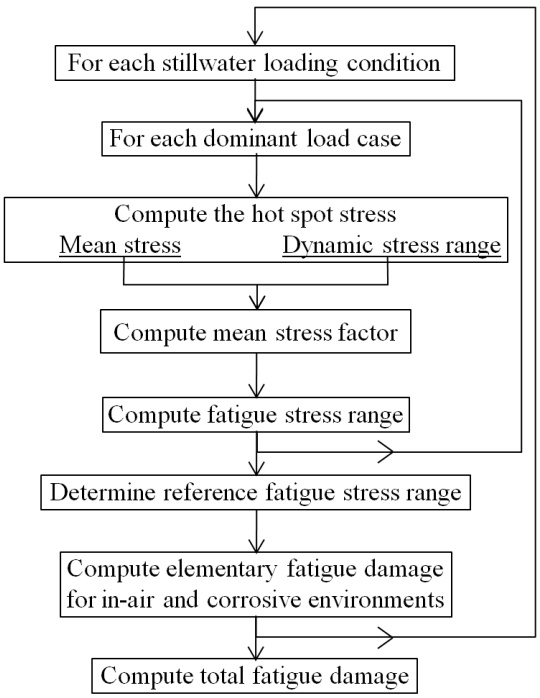

Figure 1: Flowchart of the rules fatigue assessment

At first, for each representative loading condition and for each dominant load case given by the rules [1], the fatigue stress range is computed. The rules provide a simplified stress analysis methodology to derive the hot spot stress range from the nominal stress obtained employing the beam theory. Stress concentration factors are then applied to produce the hot spot stress range. Afterwards, correction factors, including the mean stress effect, are employed to convert hotspot stress range into fatigue stress range. The rules dominant load cases have also been established using the equivalent design wave (EDW) method described in [9], so that the produced fatigue stress range are expected to be the long term value at a probability level P=10^{-2}.

Then, the reference fatigue stress range ($\Delta\sigma_{FS}$) is determined as the maximum value over the 5 dominant fatigue load cases provided by the rules. The long term stress distribution is then represented by a two-parameter Weibull distribution for which the shape factor is set as unity and Eq. (1) can compute the scale factor k.

$$k = \Delta\sigma_{FS} \big/ ln\left(10^2\right) \tag{1}$$

The elementary fatigue damages can thus be evaluated by the mean of SN curves for each:

- representative loading condition:
  -full load, 50% of design life
  -normal ballast, 50% of design life
- and type of environment using the appropriate SN curves:
  -in-air environment, for which the protection coating is effective, 80% of design life
  -corrosive environment, 20% of design life

, as provided by the rules.

Finally, the Miner's sum in Eq. (2) can produce the total fatigue damage D_{tot} by combining the elementary damages weighted by their fraction of life time in each loading condition and type of environment.

$$\begin{aligned} D_{tot} = {} & 80\%\left(50\%D_{Air,Full} + 50\%D_{Air,Ballast}\right) \\ & + 20\%\left(50\%D_{Corr,Full} + 50\%D_{Corr,Ballast}\right) \end{aligned} \tag{2}$$

CR Classification Society (CR) developed the software named HighCRest to verify the

compliance of the ship structural scantling with the rules [1] prescriptive requirements, including the fatigue life assessment. Figure 2 presents the midship section examined using this software.

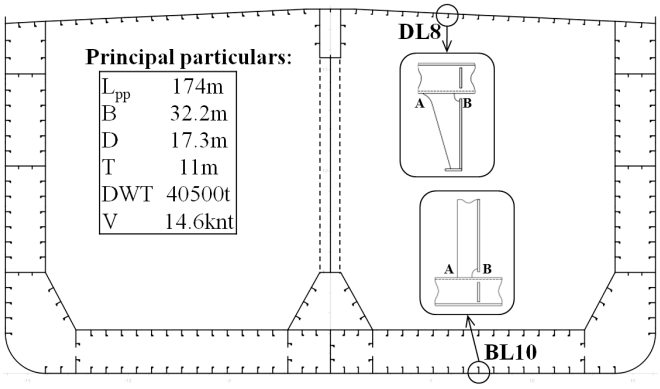

Figure 2: Oil tanker midship section

Amongst all the longitudinals end connections in the midship section, this study has selected two of them for further analyses, based on the high fatigue damage assessed at their toe (A, see Fig.2):

- the deck longitudinal No.8 (DL8, see Fig.2) has a fatigue damage of 0.827
- the bottom longitudinal No.10 (BL10, see Fig.2) has a fatigue damage of 1.314

Table 3 presents the detailed results in terms of stresses and elementary fatigue damages for this approach referenced as the method ①.

2.2 DIRECT FATIGUE ASSESSMENT

This study evaluates by direct structural assessment the fatigue of the longitudinals DL8 and BL10. Specifically, this study employs the hydro-structure coupling software Homer edited by Bureau Veritas (BV) that can transfer directly the dynamic linear loads computed by the hydrodynamic software Hydrostar (BV) to the 3D finite element model of the full ship. For each linear load case defined by a heading and a frequency, the real and imaginary parts of the loads are transferred separately to the FE model. Afterwards, the ship static structural response is obtained by finite element analyses (FEA) that are carried out by NX Nastran. Finally, the RAO of fatigue stress can be extracted from the FEA results and the damage is evaluated by spectral fatigue analysis performed by StarSpec (BV). Figure 3 presents the flowchart of the direct fatigue assessment.

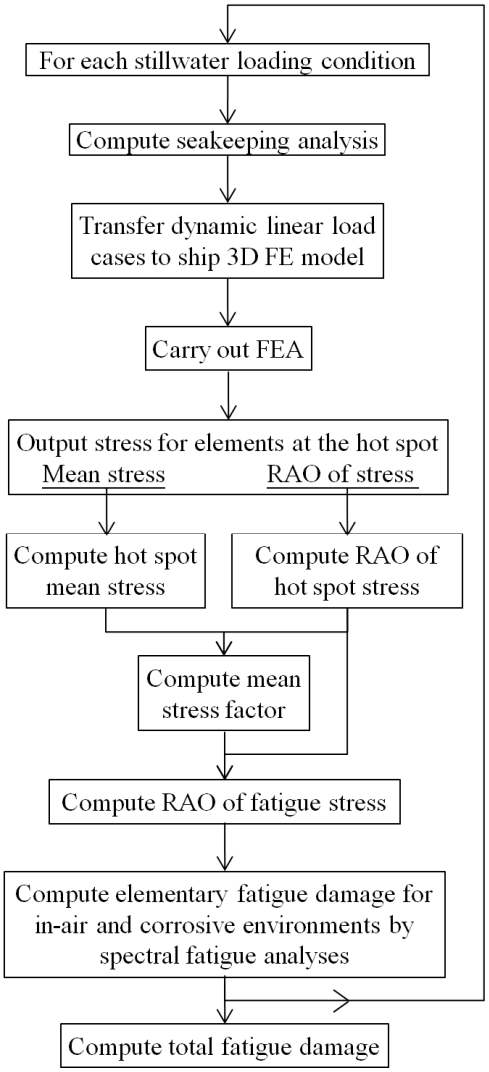

Figure 3: Flowchart of the direct fatigue assessment

This method is much more complex to execute than the rules approach. However, whereas the rules concern is to provide a methodology that can be applied to any ship, the direct fatigue assessment has for advantage to allow for examining a given ship with more precision regarding:

- the stillwater loading conditions
- the dynamic wave loads
- the structural response

Therefore, the comparison of results obtained accordingly to those two approaches enables highlighting the margins inherent to the rules.

3. HYDRO-STRUCTURE MODELING

For the direct fatigue assessment, the full ship FE model provides the mass properties. Figure 4 presents the ship FE model.

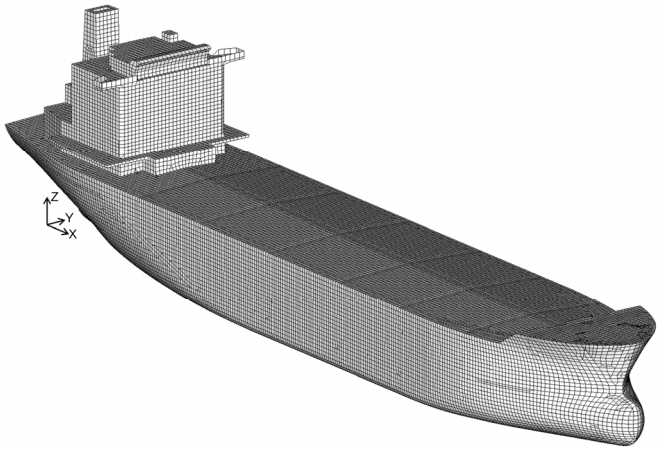

Figure 4: Ship FE model

At first, the FE model light ship weight and deadweight are calibrated to those provided by the loading manual. Additional mass elements are thus added to the structure to include the weight of equipment and cargo. Nastran RBE3 elements ensure an adequate load distribution from the mass elements to the related structural components, but it cannot reproduce the liquid pressure distribution. Therefore, for the tanks located amidship, where the fatigue is evaluated, the capacity solver of Homer is employed, so that the liquid pressure distribution can be reproduced accurately. The specific gravity and the mass of the cargo as well as the hydromesh of the tanks are thus provided. Figure 5 presents the hydromesh model of the immersed hull and cargo oil tanks No.3, 4 and 5 on both sides.

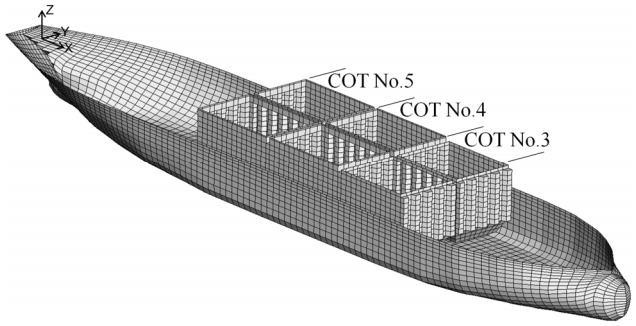

Figure 5: Hull and tanks hydro-models for the full load condition

The hydromesh enables to integrate the pressure over the modeled geometry of the hull and the tanks. Only the wetted part of the hull and the tanks are modeled. Homer can then calculate the mass and the center of gravity of the tanks. Finally, combining the FE model mass and the tanks mass, the total weight of the ship and its center of gravity can be determined.

Homer can also evaluate the hydrostatic properties of the immersed hull hydromesh. The hydro-model must be hydrostatically balanced before to run the seakeeping analysis. The offset vector between the hydro-model and the FE model coordinate systems must also be given to ensure the good transfer of loads between the two models.

Eventually, for each loading condition, the resulting stillwater bending moment distribution corresponds to that reported in the loading manual, whereas the rules stillwater bending moment for fatigue assessment is expressed as a fraction of the permissible values. Table 1 lists the stillwater bending moment considered for each loading condition and for each approach. Large deviations are produced between the two methods, especially for the ballast loading condition.

Table 1 Stillwater bending moment at the midship section

Loading condition	Stillwater bending moment *(GN.m)*		
	Rules fatigue assessment (1)	Direct fatigue assessment (2)	(2)/(1)
Full	-519.2	-630.1	121%
Ballast	801.1	363.3	45%

4. LINEAR DYNAMIC LOADS

4.1 DIRECT LOAD TRANSFER

At first, the seakeeping analysis is carried out using Hydrostar. The radiation and diffraction problems are thus solved to compute the pressures acting over the hull and in the tanks, and then to produce the ship hydrodynamic coefficients. Afterwards, the motion equations can be solved to evaluate the ship motions and accelerations.

Then, Homer can directly transfer the pressures on the structural mesh (i.e. FE model) as explained in [10]. This step is simply executed thanks to the source method employed by Hydrostar that provides a continuous representation of the potential through the wetted part of hull and tanks structural meshes. Homer can then recalculate the hydrodynamic coefficients by integrating the pressure over the hull structural mesh. Finally, the

motion equations are solved with the new coefficients. The comparison of RAOs of motion shows a good agreement between Hydrostar and Homer computations that confirms the correct loads transfer to the FE model. In addition, the FE model, when loaded, is inherently balanced as imposed by the motion equations solution.

4.2 EDW FOR FATIGUE LOADS

After carrying out the seakeeping analyses, Homer can extract the internal section forces and moments along the ship. The equivalent design wave for fatigue loads are thus determined accordingly to the method described in [9].

For DL8 and BL10 fatigue assessment, the head sea (HSM) and following sea (FSM) rules load cases are predominant. Those two load cases can produce the maximum vertical wave bending moment (M_{wv}) amidship. A spectral analysis is thus carried out to determine amidship the maximum vertical wave bending moment long term value at a probability level of 10^{-2}. Then, the RAO of vertical wave bending moment that gives the maximum long term value is selected, and the peak values for the head and the following sea are extracted with the corresponding wave frequency and phase angle. Equation (3) can compute the EDW height H_{EDW}.

$$H_{EDW} = M_{wv-LT} / RAO_{Mwv-max} \tag{3}$$

where $M_{wv\text{-}LT}$ = Maximum long term value of the vertical wave bending moment amidship and $RAO_{Mwv\text{-}max}$ = Peak value of the RAO of vertical wave bending moment that gives the maximum long term value.

The maximum EDW height over all loading conditions and dominant load cases is 2.66m. This is small compared to the ship size. Therefore, the linear load assumption is valid since the nonlinear wave load effect on the fatigue can be neglected.

The vertical wave bending moment amidship (M_{wv}), and the external and internal pressures at BL10 can then be evaluated. Equation (4) can compute the subjected loads (SL) as it relates to the considered dominant load EDW.

$$SL = RAO_{SL}(\omega_{max}) \cdot H_{EDW} \times cos(\Phi_{EDW} - \Phi_{SL}(\omega_{max})) \tag{4}$$

where $RAO_{SL}(\omega_{max})$ = RAO value of the considered subjected load taken at the frequency ω_{max} of the peak value of the dominant load RAO, H_{EDW} = the equivalent design wave height, and $\Phi_{SL}(\omega_{max})$ = phase angle of the subjected load taken at the frequency ω_{max} of the peak value of the dominant load RAO.

Table 2 presents the vertical wave bending moment amidship (M_{wv}), and the lateral pressure (P) at BL10, both evaluated by the EDW method.

Table 2 Head and following sea EDW loads for full load and normal ballast conditions

		Full		Ballast	
		M_{wv} (GN.m)	P (kN/m^2)	M_{wv} (GN.m)	P (kN/m^2)
HSM	CSR-H (1)	313.2	1.87	317.2	4.62
	EDW (2)	393.4	3.31	412.6	3.26
	(2)/(1)	126%	177%	130%	71%
FSM	CSR-H (1)	297.6	8.35	271.8	6.38
	EDW (2)	383.2	6.28	413.8	8.96
	(2)/(1)	129%	75%	152%	140%

In general, the EDW vertical wave bending moments are found approximately 30% higher than the rules values. Larger deviations are also produced regarding the pressures. However, the bottom dynamic pressure is low and thus does not affect significantly the fatigue life.

Afterwards, based on the computed EDW loads, the rules fatigue assessment (see Fig.1) is performed and the following results are obtained:

- DL8 has a fatigue damage of 1.674
- BL10 has a fatigue damage of 1.582

Table 3 presents the detailed results in terms of stresses and elementary fatigue damages for this approach referenced as the method ②.

The fatigue damages are significantly higher than those produced accordingly to the rules (see 2.1). This is discussed in 6.

5. FINITE ELEMENT ANALYSES

5.1 VERY FINE MESH FE MODELS

At first, for each stillwater loading condition and linear load cases, the global ship model FEAs are carried out and the obtained nodal displacements are extracted. Then, this study employs separate local FE models to evaluate the stress at the considered hot spots. Figure 6 presents the separate FE models.

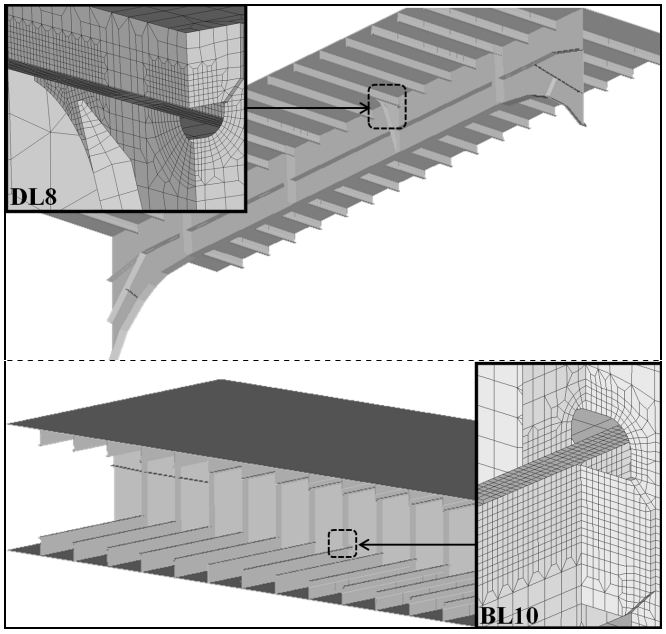

Figure 6: Deck transverse (top) and double bottom (bottom) structures FE modeling

In the local model, the hot spot areas are modelled accordingly to the very-fine-mesh rules requirements. The separate model extent is bounded by primary supporting structures. The nodal displacements obtained from the global model FE analyses are then applied to the corresponding boundary nodes on the local model. The lateral pressures are also transferred from the load files of the global model. Finally, the FEAs are carried out and for the elements surrounding the hot spot, the RAOs of stress are extracted.

5.2 STRESS OUTPUT

5.2 (a) RAO of fatigue stress

The rules provide a complete procedure to convert the stresses extracted from the elements surrounding the hot spot into the fatigue stress needed to evaluate the fatigue. Figure 3 shows the steps that can produce the RAO of fatigue stress.

At first, the rules stress interpolation method can compute the mean stress and the RAO of stress both read out at the hot spot. The correction factor for mean stress effect can then be obtained as it relates to the mean stress and the long term value of hot spot stress range. Finally, the RAO of fatigue stress is derived from the RAO of hot spot stress and corrected by various factors including that regarding the mean stress effect.

5.2 (b) Reference fatigue stress range for EDW fatigue loads

In 4.2, an equivalent design wave is obtained for each dominant load HSM and FSM. Equation (4) can thus compute the corresponding fatigue stress range response for each EDW using the RAO of fatigue stress. Afterwards, based on the produced reference fatigue stress range, the rules fatigue assessment (see Fig.1) can be performed and the following results are obtained:

- DL8 has a fatigue damage of 1.716
- BL10 has a fatigue damage of 1.250

Table 3 presents the detailed results in terms of stresses and elementary fatigue damages for this approach referenced as the method ③.

The fatigue damages are similar to those produced accordingly to the method ② (see 4.2). This is discussed in 6.

5.2 (c) Reference fatigue stress range by spectral analysis

The long term values of fatigue stress range at 10^{-2} probability level are directly evaluated by spectral analysis using the RAO of fatigue stress. The spectral analysis is carried out based on the following assumptions as provided by the rules technical background [9]:

- North Atlantic wave scatter diagram
- Pierson-Moskowitz wave spectrum
- Angular spreading of the wave energy given by the function $\cos^2$
- Equal heading probability

Afterwards, based on the produced reference fatigue stress range, the rules fatigue assessment (see Fig.1) can be performed and the following results are obtained:

- DL8 has a fatigue damage of 2.871
- BL10 has a fatigue damage of 2.332

Table 3 presents the detailed results in terms of stresses and elementary fatigue damages for this approach referenced as the method ④.

The fatigue damages are significantly higher than those produced accordingly to the method ③ (see 5.2(b)). This is discussed in 6.

6. DISCUSSION OF THE RESULTS

6.1 REFERENCE FATIGUE STRESS RANGE

This study has computed the fatigue damage and fatigue life based on the rules formulation that considers a Weibull long term distribution of the fatigue stress range scaled on the reference fatigue stress range (see 2.1). Specifically, the reference fatigue stress range is evaluated following four different methods:

- the method ① is provided by the rules and can be executed by HighCRest (see 2.1).
- the method ② is similar to the method ①, but the EDW fatigue loads are derived from hydrodynamic computations (see 4.2).
- the method ③ consists in using the hydro-structure coupling software Homer to produce the RAO of fatigue stress. Then, the EDW method can compute the fatigue stress range response (see 5.2(b)).
- the method ④ consists in performing a spectral analysis for the RAO of fatigue stress previously obtained, to produce the fatigue stress range long term value at a probability level of 10^{-2} (see 5.2(c)).

Figure 7 presents the results in terms of fatigue damage (D_{tot} , left vertical axis) and fatigue life (T_F , right vertical axis), obtained following the four methods.

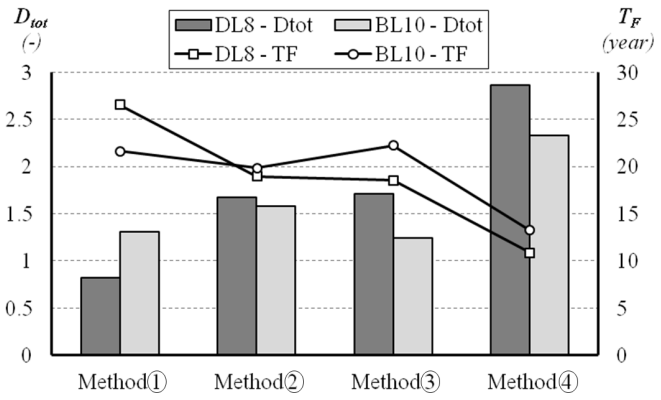

Figure 7: Fatigue evaluation by the four methods

From method ① to method ④, the evaluated total fatigue damage is increasing significantly. Specifically, the fatigue damages produced for DL8 and BL10 by the method ④ are respectively 3.47 and 1.77 times higher than those obtained by the rules (i.e. method ①). Table 3 lists the detailed results of the fatigue evaluations obtained using the four methods.

The methods ① and ② for fatigue evaluation are similar, but the dynamic loads in method ② are derived from hydrodynamic analyses by using the EDW approach. The rules loads (i.e. method ①) are derived from the same kind of EDW analyses performed for many ships. General expressions are then extracted, that can generate uncertainties. The rules technical background [9] gives a few figures that show, at the most, approximately ±10% deviation between EDW-based and rules load values examined for various ships. A correction factor is also explicitly applied to the rules [1] loads formulations. Specifically, the comparison of the loads formulations show that the rules [1] reduce by 10% the loads as initially expressed in the technical background [9]. The uncertainties due to the rules formulation and the correction factors that are explicitly applied can generate EDW-based loads higher than the rules values as shown in Table 2. In Table 3, the reference fatigue stress range and thus the fatigue damage computed by the method ② are also found much greater than those derived from the rules (i.e. method ①). Specifically, the fatigue damage produced for DL8 and BL10 by the method ② are respectively 2.02 and 1.20 times higher than those obtained by the rules. Besides, the methods ① and ② consider different values of stillwater bending moment that produce the mean stress. However, in Table 3, the factor for mean stress effect (f_{mean}) obtained by both methods is similar. Therefore, the loading condition effect on the fatigue is small.

The methods ② and ③ for fatigue evaluation consider the same EDW loads, but they employ different kinds of structural response analysis, respectively the simplified stress analysis provided by the rules, and the FEA. In Table 3, the fatigue stress and fatigue damage computed by both methods are similar. Therefore, the accuracy of the simplified stress analysis is confirmed.

Table 3 Detailed results of the fatigue evaluations obtained using the four methods

		Methods	① (See 2.2)	② (See 4.2)	③ (See 5.2b)	④ (See 5.2c)	②/①	③/②	④/③	④/①
		Static load M_{sw}	$\%M_{sw,perm}$	Loading manual						
		Static load P_s	Loading manual							
		Dynamic load	CSR-H	EDW	EDW	Direct				
		Structure response	Simplified stress analysis [1]		FEA					
DL8	Full	σ_{mean} (N/mm^2)	-63.14	-76.63	-70.96	-70.96	121%	93%	100%	112%
		$\Delta\sigma_{HS}$ (N/mm^2)	76.19	95.67	106.70	122.10	126%	112%	114%	160%
		f_{mean} (-)	0.569	0.580	0.634	0.668	102%	109%	105%	117%
		$\Delta\sigma_{FS}$ (N/mm^2)	**43.31**	**55.45**	**64.24**	**77.51**	**128%**	**116%**	**121%**	**179%**
		D_{air} (-)	0.122	0.333	0.583	1.146	273%	175%	197%	939%
		D_{corr} (-)	0.493	1.034	1.607	2.823	210%	155%	176%	573%
	Ballast	σ_{mean} (N/mm^2)	97.42	44.18	50.17	50.17	45%	114%	100%	51%
		$\Delta\sigma_{HS}$ (N/mm^2)	77.15	100.66	102.67	120.19	130%	102%	117%	156%
		f_{mean} (-)	1.000	0.940	0.949	0.942	94%	101%	99%	94%
		$\Delta\sigma_{FS}$ (N/mm^2)	**77.15**	**95.01**	**92.57**	**107.50**	**123%**	**97%**	**116%**	**139%**
		D_{air} (-)	1.128	2.294	2.103	3.441	203%	92%	164%	305%
		D_{corr} (-)	2.784	5.199	4.809	7.532	187%	92%	157%	271%
	Total	**D_{tot}** (-)	**0.827**	**1.674**	**1.716**	**2.871**	**202%**	**103%**	**167%**	**347%**
		T_F (year)	**26.6**	**19.0**	**18.61**	**10.9**	**71%**	**98%**	**59%**	**41%**
BL10	Full	σ_{mean} (N/mm^2)	-95.34	-84.77	-90.56	-90.56	89%	107%	100%	95%
		$\Delta\sigma_{HS}$ (N/mm^2)	64.99	72.84	69.53	70.87	112%	95%	102%	109%
		f_{mean} (-)	0.313	0.430	0.373	0.389	137%	87%	104%	124%
		$\Delta\sigma_{FS}$ (N/mm^2)	**20.36**	**31.65**	**24.66**	**26.19**	**155%**	**78%**	**106%**	**129%**
		D_{air} (-)	0.003	0.030	0.009	0.012	1000%	30%	133%	400%
		D_{corr} (-)	0.051	0.192	0.091	0.109	376%	47%	120%	214%
	Ballast	σ_{mean} (N/mm^2)	80.41	109.74	121.13	121.13	136%	110%	100%	151%
		$\Delta\sigma_{HS}$ (N/mm^2)	93.56	97.29	95.45	116.16	104%	98%	122%	124%
		f_{mean} (-)	0.986	1.000	1.000	1.000	101%	100%	100%	101%
		$\Delta\sigma_{FS}$ (N/mm^2)	**92.25**	**97.29**	**90.68**	**110.40**	**105%**	**93%**	**122%**	**120%**
		D_{air} (-)	2.079	2.482	1.963	3.751	119%	79%	191%	180%
		D_{corr} (-)	4.759	5.583	4.521	8.158	117%	81%	180%	171%
	Total	**D_{tot}** (-)	**1.314**	**1.582**	**1.250**	**2.332**	**120%**	**79%**	**187%**	**177%**
		T_F (year)	**21.7**	**19.9**	**22.3**	**13.3**	**92%**	**112%**	**60%**	**61%**

The methods ③ and ④ for fatigue evaluation use the direct stress assessment (see 5.2) to obtain the RAO of fatigue stress, but they employ two different approaches to determine the reference fatigue stress range. The method ③ produces the long term stress range value that relates to the EDW load, whereas the method ④ directly performs a spectral analysis to obtain the long term value at the probability level of 10^{-2}. The EDW method lies on the assumption that the maximum stress can be generated by the maximum loads, but the direct stress assessment (i.e. method ④) is inherently more accurate. In Table 3, the reference fatigue stress ranges computed by the method ④ are found approximately up to 20% higher than those derived from the method ③. Consequently, the fatigue damages produced for DL8 and BL10 by the method ④ are respectively 1.67 and 1.87 times higher than those obtained by the method ③.

6.2 LONG TERM STRESS DISTRIBUTION

This study evaluates the fatigue damage considering a long term stress distribution and a total number of cycles over the design life, both provided by the rules. Derbanne [11] shows that the long term distribution of the fatigue stress range can be accurately represented by a two-parameter Weibull distribution as given by the rules (see 2.1). Table 3 shows that the reference fatigue stress range produced by the various methods can deviate significantly from the long term value at P=10^{-2} assessed by the method ④. Figure 8 presents for DL8 and BL10 and for both loading conditions, the long term distributions of fatigue stress range produced by the spectral analysis that is carried out for the direct stress assessment (i.e. method ④).

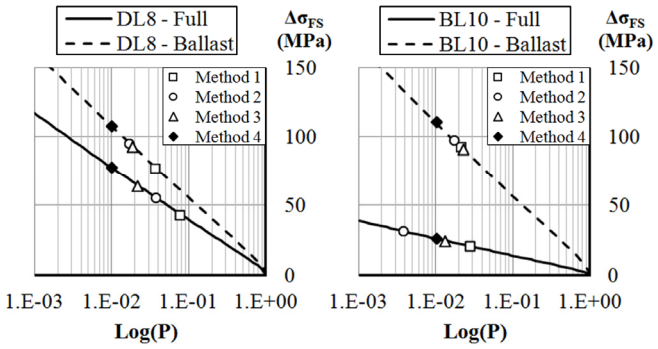

Figure 8: Probability levels associated with the reference fatigue stress ranges evaluated following the four methods

Figure 8 shows that the rules assessment (i.e. method ①) generates the largest uncertainties, since instead of producing a reference fatigue stress range at a probability level of 10^{-2}, the method ① prediction corresponds to a probability level comprised between $2.2 \cdot 10^{-2}$ and $7.6 \cdot 10^{-2}$. As a result, the long term Weibull distribution of fatigue stress range is not scaled on the right reference fatigue stress range. The fatigue damage prediction is thus affected. Particularly, because of the SN curves shape, the number of cycles to the failure varies as a function of the stress range at exponent 3 to 5. Therefore, the fatigue damage is very sensitive to the reference fatigue stress range evaluation.

As formulated in the rules, Eq. (5) can then compute the total number of cycles (N_D) over the ship design life from the duration in seagoing operation expressed in seconds.

$$N_D = f_0 \times T_D \times 365.24 \times 24 \times 3600 / 4Log(L) \quad (5)$$

where f_0 = 85% of life time in seagoing operations, T_D = 25 years design life and L = rules ship length.

The term *4Log(L)* corresponds to the mean value of the response up-crossing period that can be directly evaluated by spectral analysis. Figure 9 presents for DL8 and BL10, the ratio of the total number of cycles assessed by spectral analysis to that computed by the rules.

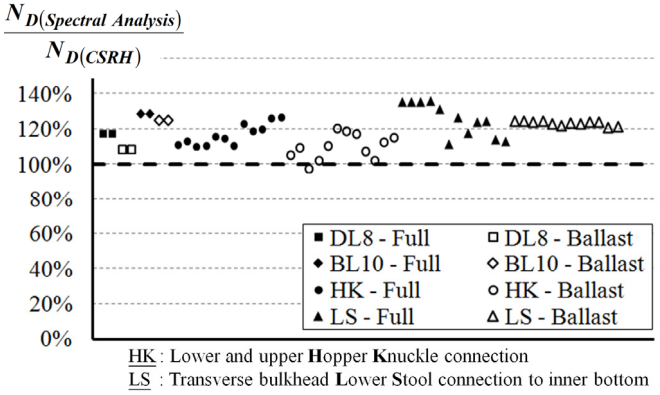

Figure 9: Total number of cycles over 25 years life comparison between spectral analysis direct calculation and CSR-H formulation

Figure 9 shows that the total numbers of cycles obtained from the spectral analysis are, in average, approximately 20% higher than those computed by the rules. This observation can be generalized to other hot spots that are analyzed in this ship, for which the ratios of total number of cycles are added in Fig.9 as those marked HK and LS. Based on the results of in total 28 hot spots all located amidship considering two loading conditions, the rules formulation can be said up to evaluate the lower bound of N_D. Therefore, the fatigue damages reported in Table 3 are all optimistic.

7. CONCLUSIONS

For two longitudinal stiffeners located in the deck and in the bottom, this study evaluates the fatigue life accordingly to the rules and by direct fatigue assessment using advanced hydro-structure coupled computations.

Compared to the rules assessment, the direct analysis generates fatigue damage 3.47 times higher for the deck longitudinal and 1.77 times

higher for the bottom longitudinal. This huge increase in terms of fatigue damage can be explained by the following observations:

- The rules loads are smaller than the equivalent design wave loads derived from hydrodynamic analyses. The rules loads are obtained based on the same EDW analyses performed for many ships. However, the rules general expressions can generate uncertainties in the range of approximately ±10%. Correction factors are also explicitly applied in the rules to reduce by 10% the loads as initially expressed in the technical background [9].
- The EDW approach lies on the assumption that the maximum stresses can be generated by the maximum loads. However, considering the same RAO of fatigue stress, the reference fatigue stress range value that relates to the EDW load is approximately up to 20% smaller than that directly produced by spectral analysis.
- For 28 various hot spots all located amidship, the total number of cycles over the ship design life obtained by spectral analysis is, in average, approximately 20% higher than the rules prediction.

Based on those observations, it can be concluded that at each level of the rules fatigue assessment, the evaluation of the loads, the stresses and the fatigue damages are reduced compared to a direct fatigue assessment considering the rules assumptions. Especially, because of the SN curves shape, the fatigue damage is very sensitive to the fatigue stress range evaluation. Besides, the results show that the stillwater loads as expressed by the rules have a very limited effect on the fatigue compared to real loading conditions.

The inaccuracy of the computations performed for this study, especially regarding the hydrodynamic analyses, can partly explain those deviations. Because the hydrodynamic software here employed is of the same kind as those used by the IACS members for the rules development, the deviations are thus supposed to be mostly due to the ability of the IACS to calibrate the results on real data. The conservative assumption of the North Atlantic wave environment can also generate overestimated loads compared to validated practices that can partly explain why the IACS lowers explicitly the level of loads.

Finally, this study enables highlighting the margins taken by the IACS to calibrate the numerical computations based on the experience accumulated over the years by numerous classification societies with the pre-CSR and CSR ships, as well as with the "FPSO fatigue capacity JIP". A comprehensive understanding of the IACS experience could also be extracted by extending the scope of this study to more hot spots for more structural details in more ships.

REFERENCES

1. IACS, 2014 ‘Harmonized Common Structural Rules for Bulk Carriers and Oil Tankers’, *IACS, London.*
2. IMO, 2010 ‘Adoption of the international goal-based ship construction standard for Bulk Carriers and Oil Tankers’, *MSC.290(87), Maritime Safety Committee (MSC).*
3. IACS, 2014 ‘Uncertainties Related to the Fatigue Assessment Procedure’, *Technical Background Report for the CSR-H, IACS, London.*
4. S. Maddox, 2001 ‘Recommended design S-N curve for fatigue assessment of FPSOs’, *11th ISOPE, Stavanger.*
5. W. Fricke, 2001 ‘Recommended hot spot analysis procedure for structural details of FPSOs and ships on round robin FE analysis’, *11th ISOPE, Stavanger.*
6. I. Lotsberg, 2006 ‘Fatigue design of plated structures using finite element analysis’, *Journal of ship and offshore structures, Vol. 1, pp. 45-54.*
7. I. Lotsberg et al, 2008 ‘A procedure for fatigue design of web-stiffened cruciform connections’, *SAOS, Vol. 3, pp. 113-126.*
8. IACS, 2014 ‘Hull Girder Vibration’, *Technical Background Report for the CSR-H*, *IACS, London.*
9. IACS, 2014 ‘Equivalent Design Wave (EDW) for Fatigue Loads’, *Technical Background Report for the CSR-H, IACS, London.*
10. S. Malenica, et al, 2009 ‘Some aspects of hydro-structure coupling for combined action of seakeeping and sloshing’, *28th OMAE, Honolulu, USA.*
11. Q. Derbanne et al, 2011 ‘Evaluation of Rule-Based Fatigue Design Loads Associated at a New Probability Level’, *21st ISOPE, Hawaii, USA.*